Published in "Development 142(11): 1992–2001, 2015"
which should be cited to refer to this work.

Phyllotaxis involves auxin drainage through leaf primordia

Yamini Deb[1], Dominik Marti[2,*], Martin Frenz[2], Cris Kuhlemeier[1] and Didier Reinhardt[3,‡]

ABSTRACT

The spatial arrangement of leaves and flowers around the stem, known as phyllotaxis, is controlled by an auxin-dependent reiterative mechanism that leads to regular spacing of the organs and thereby to remarkably precise phyllotactic patterns. The mechanism is based on the active cellular transport of the phytohormone auxin by cellular influx and efflux carriers, such as AUX1 and PIN1. Their important role in phyllotaxis is evident from mutant phenotypes, but their exact roles in space and time are difficult to address due to the strong pleiotropic phenotypes of most mutants in phyllotaxis. Models of phyllotaxis invoke the accumulation of auxin at leaf initials and removal of auxin through their developing vascular strand, the midvein. We have developed a precise microsurgical tool to ablate the midvein at high spatial and temporal resolution in order to test its function in leaf formation and phyllotaxis. Using amplified femtosecond laser pulses, we ablated the internal tissues in young leaf primordia of tomato (*Solanum lycopersicum*) without damaging the overlying L_1 and L_2 layers. Our results show that ablation of the future midvein leads to a transient accumulation of auxin in the primordia and to an increase in their width. Phyllotaxis was transiently affected after midvein ablations, but readjusted after two plastochrons. These results indicate that the developing midvein is involved in the basipetal transport of auxin through young primordia, which contributes to phyllotactic spacing and stability.

KEY WORDS: Phyllotaxis, Patterning, Meristem, Laser ablation, Auxin, PIN1, Tomato

INTRODUCTION

Leaves and flowers are arranged in regular patterns around the stem, a phenomenon known as phyllotaxis (Reinhardt, 2005; Kuhlemeier, 2007). Most frequent is spiral phyllotaxis, in which the divergence angle between successive lateral organs is close to the golden angle of 137°, but alternate (distichous), opposite (decussate) and whorled arrangements are also common. Leaves and flowers initiate from the shoot apical meristem, a small dome of cells that harbors a pool of stem cells in its center (central zone). The central zone is surrounded by the peripheral zone, a ring-shaped domain with cells that have the potential to initiate the lateral organs. All theories of phyllotaxis agree that the position of an incipient primordium is in some way determined by the position of previously initiated primordia. A century ago, Schoute proposed a conceptual model in which an inhibiting substance is produced by the previously initiated organ primordia; when such an inhibitor diffuses into the meristem, a new initial will arise in the peripheral zone at the lowest inhibitor concentration (Schoute, 1913). Mathematical models in which the concentration of the inhibitor decreases with time and distance can reproduce all commonly observed phyllotactic patterns (Smith et al., 2006a). Such models, however, do not shed light on the underlying molecular circuitry.

Over the past decade the plant hormone auxin has been firmly established as a central regulator of phyllotaxis. Auxin is distributed in the tissue in complex patterns that reflect and predict the patterns of organ initiation (Benková et al., 2003; Reinhardt et al., 2003b; Heisler et al., 2005; Bayer et al., 2009). The earliest indication of organ initiation is the formation of an auxin maximum in the epidermis of the meristem, also known as the L_1 layer. It is thought that the two youngest primordia (P_1, P_2) drain auxin from the meristem and thereby determine the position of the incipient primordium (I_1). Thus, auxin acts as an inducer of organ formation, and the postulated inhibitory fields around pre-existing primordia reflect low auxin concentrations in their vicinity (Reinhardt, 2005; Kuhlemeier, 2007).

In contrast to other mobile signals, the gradients of auxin are set up by directional transport from cell to cell by a mechanism known as polar auxin transport. Three families of auxin transporters control the distribution of auxin in various tissues of the plant body. The AUX1/LAX proteins are influx carriers (Swarup and Peret, 2012), whereas cellular auxin efflux is mediated by two distinct groups – the PIN proteins (Krecek et al., 2009) and a subgroup of ABC transporters (Kang et al., 2011). In concert, these auxin transporters create spatially precise auxin gradients that direct morphogenesis in the root and the shoot (Zazimalova et al., 2010). Indeed, the distribution and subcellular polarization of PIN1 in the L_1 layer correctly predict the position of the future primordium (de Reuille et al., 2006).

For auxin flux to be directed through dozens to hundreds or even thousands of cells, the subcellular polarity of the transporters needs to be precisely coordinated throughout a tissue (Berleth and Sachs, 2001). In computational models, the polarization of PIN1 is accomplished by a positive feedback between auxin and the efflux carrier PIN1, the molecular mechanism of which is as yet unknown. Early computational models propose that PIN1 preferentially localizes towards neighboring cells with higher auxin concentration (‘up-the-gradient’ polarization) (Jönsson et al., 2006; Smith et al., 2006b). The dynamic model proposed by Smith et al., which is implemented on a realistic cellular template of dividing cells, generates correctly positioned auxin maxima in the L_1 and recreates the common phyllotactic arrangements such as spiral, distichous and decussate; it also recapitulates the effects of surgical manipulations and mutant phenotypes (Smith et al., 2006b).

The auxin maximum in the L_1 is thought to induce the formation of the future midvein, which subsequently serves as a conduit for auxin drainage and thereby positions the next primordium. Convergence point formation and initiation of the midvein must be well coordinated to secure stable organ positioning. In fact,

[1]Institute of Plant Science, University of Bern, Bern 3013, Switzerland. [2]Institute of Applied Physics, University of Bern, Bern 3012, Switzerland. [3]Department of Biology, University of Fribourg, Fribourg 1700, Switzerland.
*Present address: DTU Fotonik, Technical University of Denmark, Roskilde 4000, Denmark.

‡Author for correspondence (didier.reinhardt@unifr.ch)

these two processes occur almost simultaneously during early stages of organogenesis (Bayer et al., 2009). The importance of stabilization of the core mechanism was recently underscored by the discovery of a cytokinin-dependent mechanism that suppresses premature outgrowth of I_1 (Besnard et al., 2014). The midvein as a conduit for auxin drainage might represent another stabilizing mechanism.

Vein formation has been studied in considerable detail at later stages of leaf development (Sauer et al., 2006; Scarpella et al., 2010; Sawchuk et al., 2013). It is thought to proceed by canalization (Sachs, 1981), a process in which auxin becomes gradually focused into narrow channels. Experimental data and mathematical modeling of canalization suggest that during formation of the midvein in the inner tissues (L_2 and L_3) PIN1 is not polarized 'up-the-gradient' as in convergence point formation in L_1, but by a flux-dependent mechanism. Thus, phyllotaxis might require two different mechanisms for PIN1 polarization that need to act simultaneously in a 3D patterning process.

We have proposed a computational model in which the mechanism of PIN1 polarization in each cell depends on the auxin concentration in that same cell. Such a model can both create an auxin convergence point in the L_1 and produce a gradually narrowing file of auxin-transporting cells with high auxin levels in the internal tissue (Bayer et al., 2009). The model also recapitulates the complex patterns of PIN1 polarization. Genetic analyses have recently provided support for such a dual polarization model (Kierzkowski et al., 2013; Furutani et al., 2014).

Here, we aimed to address the role of the inner tissues by specifically interfering with midvein formation at early stages of primordium formation in P_1. Genetic interventions in the meristem often produce pleiotropic mutant phenotypes that are difficult to interpret. Therefore, we resorted to tissue ablation, an alternative to genetic interference with a long tradition in meristem research (Pilkington, 1929; Snow and Snow, 1931, 1933; Sussex, 1951). More recently, laser-based ablation in combination with confocal laser microscopy and live imaging has been used as a precision tool to address organogenesis and patterning, both at the shoot and the root apex (van den Berg et al., 1995, 1997; Reinhardt et al., 2003a, 2005; Xu et al., 2006; Depuydt et al., 2013). The challenge we faced was how to perform robust ablations of internal meristem cells in a dense tissue with strong light scattering without damaging the overlying L_1 and L_2 layers.

To this end, we designed a custom nanosurgery system consisting of a femtosecond laser beam optically coupled into a confocal microscope. This allowed us to perform defined disruptions of selected individual cells in subepidermal tissue layers and, at the same time, high-resolution imaging and optical 3D sectioning in the same integrated system, with high optical penetrance through the dense tissues of the shoot apical meristem. Femtosecond laser pulses interact with the tissue through a nonlinear process resulting in short-lived confined interactions that comprise just the focal volume of the tightly focused laser beam, thus offering unprecedented ablation precision. This system offered the novel potential to image the 3D cellular structure of the meristem, selecting and ablating the target L_3 cells and to observe the cellular response to the induced damage by imaging the same cells before and at various times after the ablations. Since the nonlinear interaction is localized in the beam focus and rapidly dissipates without interfering with surrounding cells, direct internal ablation of L_3 cells is possible without affecting the L_1 and L_2 layers above. The degree and extent of cell damage were controlled by varying the single pulse energy and/or the number of pulses applied per cell. After the highly localized ablations, which did not affect the overall vitality of the apices, the further development of the apices was live-imaged and analyzed for subtle quantitative phenotypes in organ initiation and primordium growth.

With this nanosurgery system, we tested the prediction that the incipient midvein plays an important role in defining organ size and position. We ablated the cells in P_1 that express PIN1, thereby ablating the developing midvein in the center of the primordia. We show that this transiently increased the area expressing DR5:YFP, indicative of an overaccumulation of auxin in the ablated primordia. Consistent with this notion, ablated primordia grew wider than non-ablated controls. Surprisingly, ablated primordia did not suffer from any long-term consequences of the destroyed incipient midvein, conceivably because a new midvein was initiated within a few days. Taken together, our results indicate that the cells of the future midvein have a function in auxin drainage. Hence, we provide the first evidence for the direct role of the midvein in phyllotactic patterning, a prediction that emerged from recent modeling studies (Bayer et al., 2009).

RESULTS

Effects of ablation of the incipient midvein on PIN1-GFP expression and primordium development

To test the role of the incipient midvein in organogenesis and phyllotaxis, we chose the early P_1 stage, i.e. after local induction of PIN1 in deeper layers and after the initiation of primordium growth, but before the histological definition of the future midvein (Fig. 1A). This stage is known as the preprocambial stage of vascular development (Kang and Dengler, 2004; Scarpella et al., 2004). Although PIN1 was already clearly induced at this stage, it

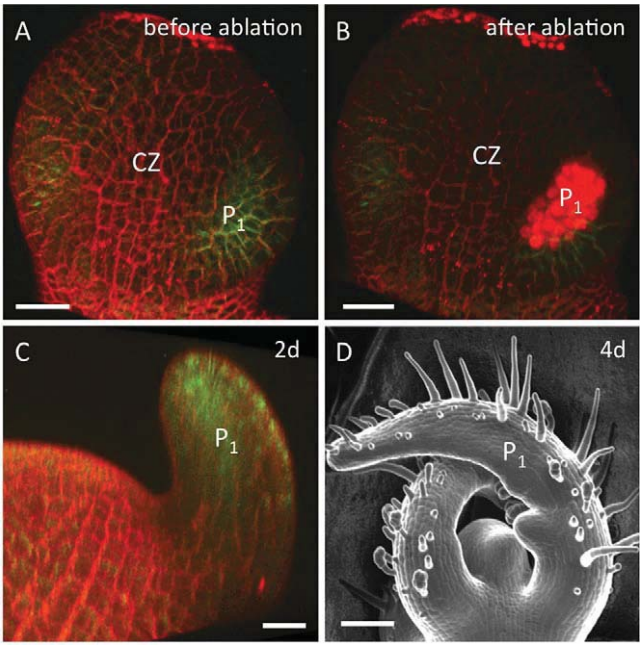

Fig. 1. Laser ablation of the incipient midvein tissue at P_1. (A) Tomato apex in top view showing the meristem with its central zone (CZ) and the youngest primordium (P_1). Cells of the developing midvein can be identified by their expression of PIN1-GFP (green). (B) Laser ablation of the PIN1-GFP-expressing cells is revealed by strong nuclear staining with propidium iodide (red). (C) Tomato apex 2 days after ablation of the incipient midvein of P_1, which has further developed. (D) Tomato apex 4 days after ablation of the incipient midvein of P_1, which has developed into a normal leaf primordium. Images in A-C represent maximum intensity projections. Scale bars: 25 µm in A-C; 100 µm in D.

was not yet restricted to a narrow cell file (Fig. 1A). The expression domain of PIN1, as well as the accumulation of propidium iodide, was used to evaluate the efficiency and precision of the ablations in the developing midvein, and as a marker to follow the subsequent initiation and development of a new midvein. Laser ablation removed PIN1 expression at this site, just leaving the low-level PIN1-GFP expression in the surrounding cells that is characteristic for meristematic cells (Fig. 1B). These results indicate that the incipient midvein has been removed, but that the adjacent cells are alive. Despite the ablation of the future midvein, primordium development continued normally (Fig. 1C) and resulted in leaf primordia that were indistinguishable from untreated leaf primordia (Fig. 1D). Ablations at a different site nearby P_1 did not affect PIN1 expression or development at P_1 (data not shown).

In order to address the fate of the developing midvein and its potential recovery after ablation, a timecourse experiment was performed. After midvein ablation, apices were live-imaged in 6-h intervals for 48 h and examined for PIN1-GFP expression (Fig. 2). Counterstaining with propidium iodide showed that the lesions were only transiently visible (Fig. 2B-E). Already at 6 h after ablation, the size of the lesion was reduced, and by 24-48 h after ablation it had disappeared entirely (Fig. 2F-J). These results suggest that the ablated cells become compressed and that neighboring cells and their progeny take over the respective volume. Concurrently, PIN1-GFP expression recovered, and assumed an even larger area than before the ablations (Fig. 2D-G), compared with control apices (Fig. 3). Precise determination of the size of the PIN1-GFP domain was not possible because of the constitutive expression of PIN1 in the surrounding meristem cells (Reinhardt et al., 2003b; Heisler et al., 2005), which prevents precise delimitation of the area of increased PIN1 expression.

In order to examine the phenomenon in the longitudinal dimension, the images of ablated apices were subjected to 3D reconstructions based on *z*-stacks from the timecourse experiment (Fig. 2). Virtual longitudinal sections showed that, after ablation of the incipient midvein, PIN1-GFP remained expressed in the L_1 and L_2 layers (Fig. 4), showing that the lesions were confined to the L_3 layer. Consistent with the analysis of transverse sections (Fig. 2), the lesions disappeared after ablation, and a new PIN1-expressing domain appeared on the adaxial side of the lesion, i.e. towards the meristem center (Fig. 4B-F). Subsequently, the PIN1-GFP domain expanded downwards (Fig. 4G-K), indicating that a new preprocambial strand had been established. Ultimately, ablated primordia developed into normal leaves (Fig. 4L).

Effects of incipient midvein ablation on the DR5:YFP expression domain and primordium development

In order to explore potential changes in auxin distribution that might result from ablation of the developing midvein, we monitored expression of the auxin response marker DR5:YFP, which is commonly used as a proxy for auxin concentration (Brunoud et al., 2012). A nuclear-localized variant of YFP was chosen to provide a strong signal and clearly defined expression domains (Shani et al., 2010). In transverse optical sections, a prominent region of DR5:YFP expression was observed at the tip of P_1 (Fig. 5A). After ablation, the area of this domain remained approximately similar for 6 h (Fig. 5B,C); however, from 12 h onwards the DR5 expression domain (hereafter referred to as the DR5 domain) widened significantly (Fig. 5D-J, compare with Fig. 6), indicating that ablation of the midvein resulted in the enhanced accumulation of auxin.

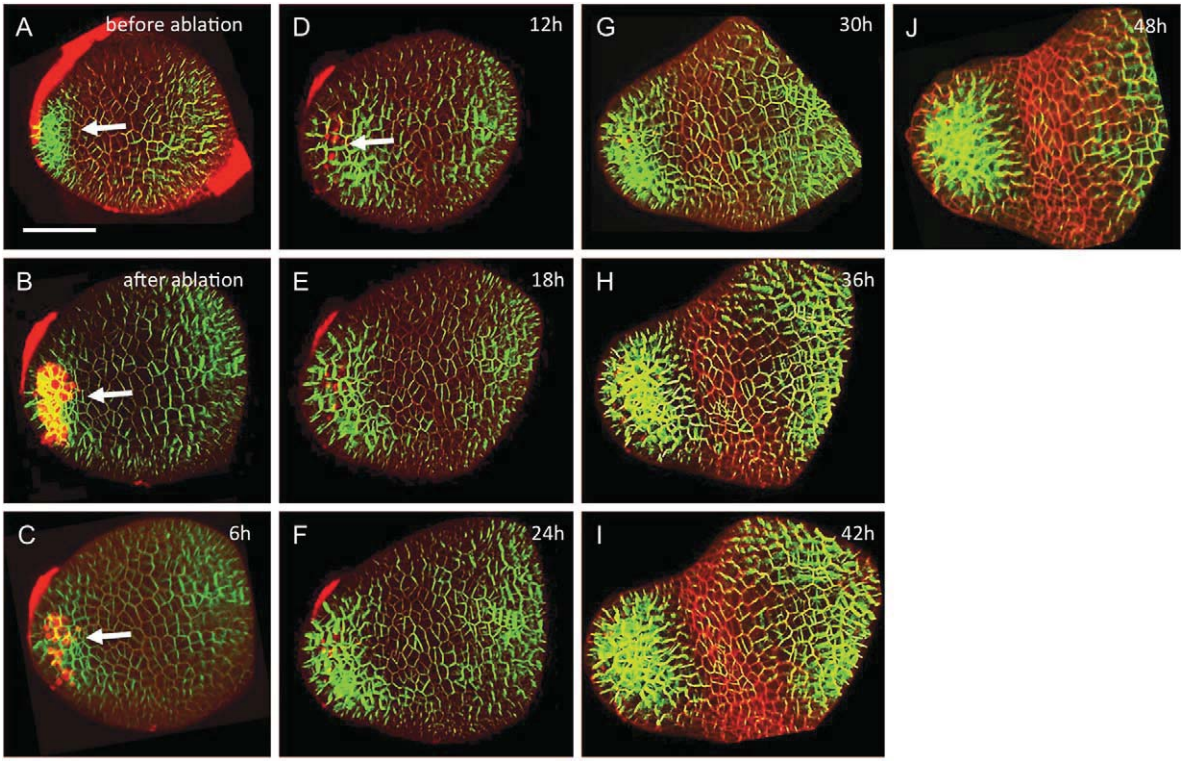

Fig. 2. Development of the apex and expression of PIN1-GFP after ablation of the incipient midvein of P_1. A tomato apex of the line expressing PIN1-GFP is shown in transverse optical section before ablation (A), just after ablation (B), and 6 (C), 12 (D), 18 (E), 24 (F), 30 (G), 36 (H), 42 (I) and 48 (J) h after ablation of the midvein at P_1 (arrow). Note the wider expression domain of PIN1-GFP 24 h after ablation (F), as compared with the situation before ablation (A). Images represent maximum intensity projections. Scale bar: 50 μm.

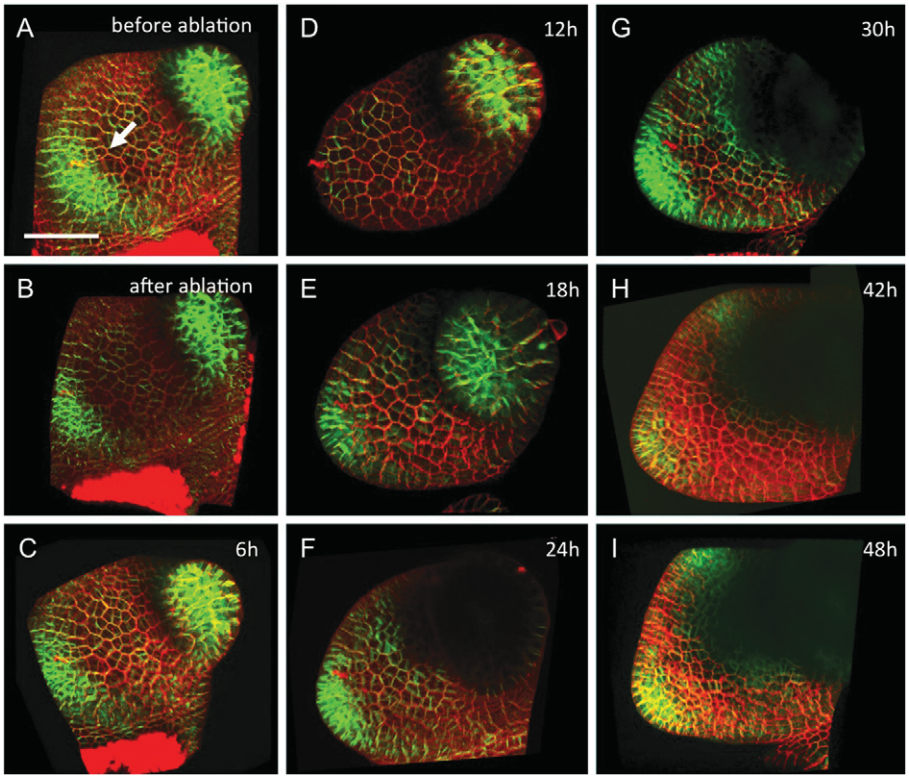

Fig. 3. Development of a PIN1-GFP control apex without ablation. An apex of the PIN1-GFP tomato line are shown in transverse optical section before (A) and just after (B) mock ablation, and 6 (C), 12 (D), 18 (E), 24 (F), 30 (G), 42 (H) and 48 (I) h after mock ablation of the midvein at P_1 (arrow). All parameters are as in Fig. 2, except that the ablation was omitted. To ensure comparable treatments, the apices were imaged before and after the mock ablation. Images represent maximum intensity projections. Scale bar: 50 µm.

Consistent with the increase of the DR5 domain, the area of high PIN1-GFP expression in P_1 was increased (Fig. 7A); however, the differences could not be quantified because the area of induced expression at P_1 could not be delimited with confidence owing to the gradual, rather than distinct, difference in PIN1 expression between P_1 and the surrounding tissues (Fig. 7A). By contrast, the area of the DR5 domain was clearly delimited (Fig. 7A), allowing its quantification (see Materials and Methods). The area of the DR5 domain at P_1 in control apices did not change significantly over the entire experimental period; however, the ablated apices exhibited significantly enlarged DR5 domains between 12 and 30 h after ablation (Fig. 7B, crosses), relative to the beginning of the experiment. Consistently, pairwise comparison between ablated apices and controls at the different time points revealed a significant increase of the DR5 domain between 6 and 30 h (except for 24 h). Hence, the DR5 domain transiently expanded after midvein ablations, but returned to normal size after 36 h (Fig. 7B).

Size of leaf primordia after ablation of the incipient midvein

The area of the auxin peak at sites of primordium formation is thought to define the width of the primordia, and, indeed, addition of auxin to young primordia at the early P_1 stage increases their size (Reinhardt et al., 2000). We measured whether the width of primordia was affected by midvein ablation and by the resulting increase in the DR5 domain. In the PIN1-GFP line, ablation of the future midvein caused a significant widening of the primordia after 24 h (Fig. 8A). Similarly, in the DR5:YFP line, ablated primordia were significantly wider, an effect that was already observed at 6 h and onward (Fig. 8B). However, we note that the effect was transient because leaves were normal at later stages, indicating that postmeristematic growth compensated for differences in primordium size.

Phyllotactic development after ablation of the incipient midvein

Changes in primordium position or size are likely to affect the positioning of subsequent primordia; hence, we determined the phyllotactic angles between P_1 and the successive primordia after midvein ablation. Whereas the phyllotactic angles in control apices were always in the range between 130° and 145° (data not shown), the angles after midvein ablation became more variable (Fig. 9). Only ~37% of the two successive primordia (I_1 and I_2) were positioned with a divergence angle between 130° and 145° from the previous primordium, with the remainder showing either a larger or a smaller divergence angle with no clear tendency (Fig. 9). The following divergence angle between I_2 and I_3, however, was entirely normal, showing that the perturbations of phyllotaxis after midvein ablation were transient (Fig. 9).

DISCUSSION

Experimental and mathematical analysis of phyllotaxis – from 2D to 3D

The first auxin-based models explained phyllotaxis as an essentially 2D phenomenon that is restricted to the outermost cell layer of the meristem (Kuhlemeier, 2007). Indeed, the earliest steps in phyllotactic patterning seem to be related to the L_1 layer (Benková et al., 2003; Reinhardt et al., 2003b; Heisler et al., 2005), and computational models of phyllotaxis are able to recreate various natural phyllotactic patterns in 2D sheets of cells (Jönsson et al., 2006; Smith et al., 2006b). Consistent with this view, recent evidence showed that expression of PIN1 in the L_1 layer is sufficient to produce normal phyllotactic patterns (Kierzkowski et al., 2013) as long as additional stabilizing factors, such as auxin influx carriers, contribute to PIN1 function (Bainbridge et al., 2008; Kierzkowski et al., 2013). Nevertheless, combined experimental and theoretical analysis has suggested that phyllotactic mechanisms cannot be fully understood without the internal cell layers – in

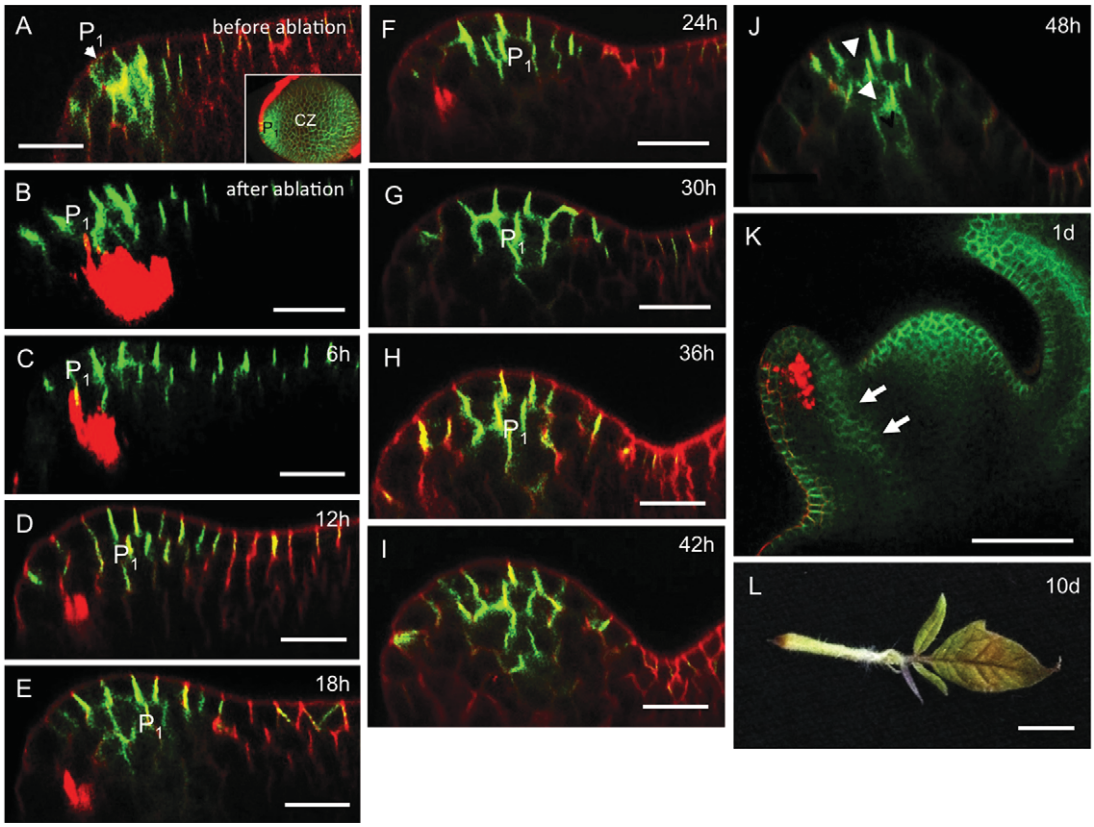

Fig. 4. Development of the apex and expression of PIN1-GFP after ablation of the incipient midvein of P_1. (A-J) 3D image stacks from the apex shown in Fig. 2 were reconstructed to generate virtual longitudinal sections. A tomato apex of the line expressing PIN1-GFP is shown before ablation (A), just after ablation (B), and 6 (C), 12 (D), 18 (E), 24 (F), 30 (G), 36 (H), 42 (I) and 48 (J) h after ablation of the incipient midvein at P_1. P_1 denotes the young primordium in A-C and the shifted new convergence point after the ablation in D-H. Arrowheads (J) indicate the newly established secondary midvein. (K) Longitudinal overview over an entire apex 1 day after ablation of the incipient midvein. Note the newly established file of PIN1:GFP-expressing cells (arrows) on the adaxial side of the lesion. (L) P_1 10 days after midvein ablation. Images in A-K represent maximum intensity projections. Scale bars: 25 µm in A-J; 50 µm in K; 5 mm in L.

particular, the canalization of auxin through the developing midvein of young primordia is predicted to have a central role in the patterning of the apex – hence introducing the third dimension into models of phyllotaxis (Bayer et al., 2009). Clearly, PIN1 acts in concert with additional factors that operate in the L_1, but also in deeper layers of the meristem (Bainbridge et al., 2008; Robert and Offringa, 2008; Furutani et al., 2014).

Exploring the role of the developing midvein in phyllotaxis

Based on the proposed role of primordia as auxin sinks that drain auxin from surrounding tissues and remove it from the meristem through the developing midvein (Reinhardt et al., 2003b; Bayer et al., 2009), ablation of the incipient midvein would be predicted to interfere with the removal of auxin from the meristem. This, in turn, would affect the treated primordia directly, and could potentially interfere with the positioning of further organ primordia. The fact that midvein ablation led to a transient expansion of the DR5 domain indicates that, indeed, the ablations caused auxin to accumulate in the tissues above the ablation. Consistent with this interpretation, the primordia became wider after ablations. The perturbations around the ablations, and the scar itself, were transient, suggesting that functionally equivalent cells replaced the ablated tissue. Indeed, new cell files marked by PIN1-GFP developed next to the lesions within one day, presumably functionally replacing the former incipient midvein tissue (Fig. 4). This highlights the remarkable capacity of plants to repair damage (Sachs, 1981; Sauer et al., 2006).

The relationship between vascular development and leaf formation was addressed decades ago by detailed microscopy analysis. In most species, the spatial organization of the vasculature in the shoot apex is strictly correlated with phyllotactic patterns (Kirchoff, 1984), and expression analysis of the early procambial marker *HOMEOBOX GENE 8* in *Arabidopsis thaliana* has supported these findings (Kang et al., 2003). Hence, vascular development and organ formation are closely correlated. The fact that pre-existing vascular strands in the apex of *Populus deltoides* pointed to the site of incipient leaf formation before the primordia had emerged has been taken as evidence that vascular strands could predict, or even direct, leaf formation (Larson, 1975). However, despite the strong relationship between organogenesis and initiation of the first vascular strand, the causal relationship and the exact sequence of events are difficult to establish, even with the earliest molecular markers and with modern genetic and microscopy tools, because the two phenomena overlap to a large extent (Bayer et al., 2009). Hence, it is possible that the initiation of primordium growth and the differentiation of the first central vascular strand represent two parallel processes that have a common basis (auxin), rather than being two sequential events where one directs the other.

Interactions between the L_1 surface layer and internal tissues

Despite the extended lesion in its center, P_1 did not degenerate after midvein ablation. The relatively mild and transient effects of

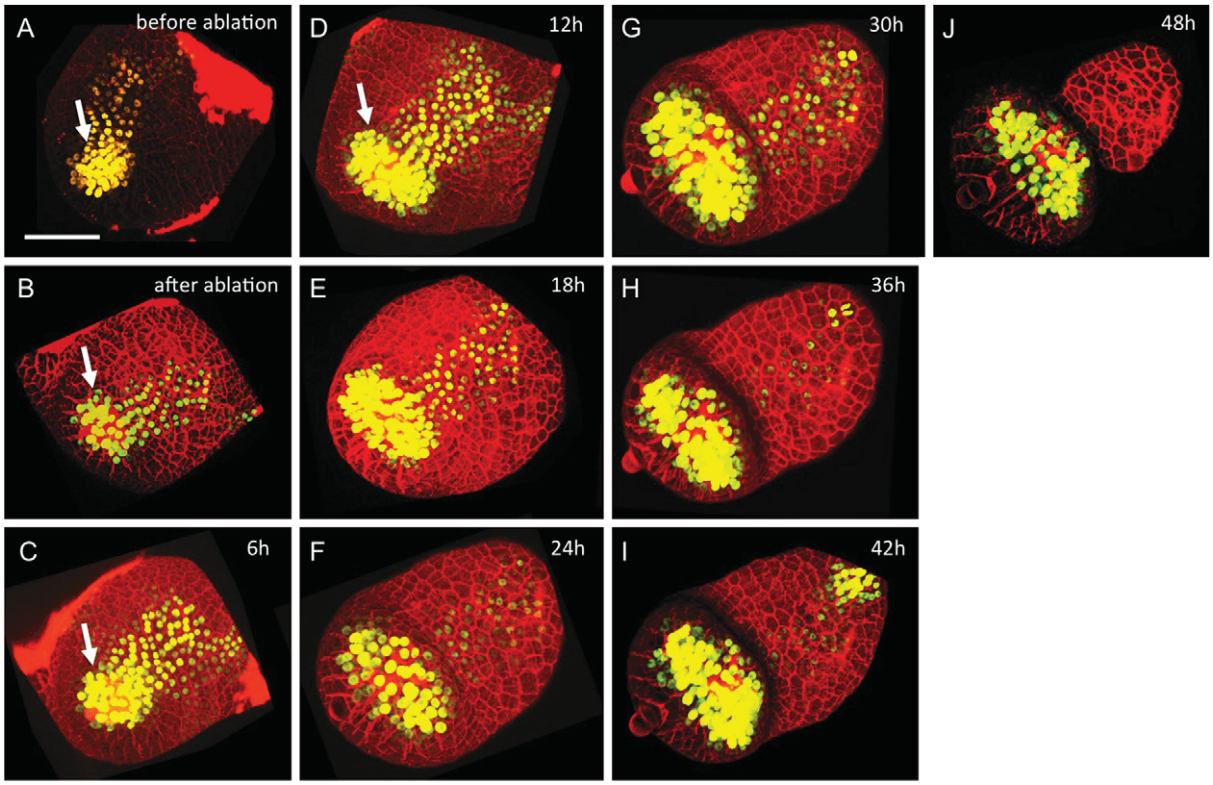

Fig. 5. Induction of DR5:YFP at P_1 after ablation of the incipient midvein. An apex of the DR5:YFP tomato line was treated as in Fig. 2. Images show an apex before (A) and after (B) ablation, and 6 (C), 12 (D), 18 (E), 24 (F), 30 (G), 36 (H), 42 (I) and 48 (J) h after ablation of the midvein at P_1. The arrow (A-D) points to the P_1-related auxin peak revealed by DR5:YFP (DR5 domain). Note the widening of the DR5 domain between 6 h (C) and 12 h (D) after ablation. Images represent maximum intensity projections. Scale bar: 50 µm.

midvein ablations might at first appear surprising. Indeed, the P_1 grew even wider after midvein ablations compared with controls (Figs 7 and 8). Similarly, the effect on phyllotaxis was mild and transient (Fig. 9). While these findings allowed us to appreciate the impressive regenerative capacities of the meristem tissues, these results also confirm the central importance of the L_1 layer in the

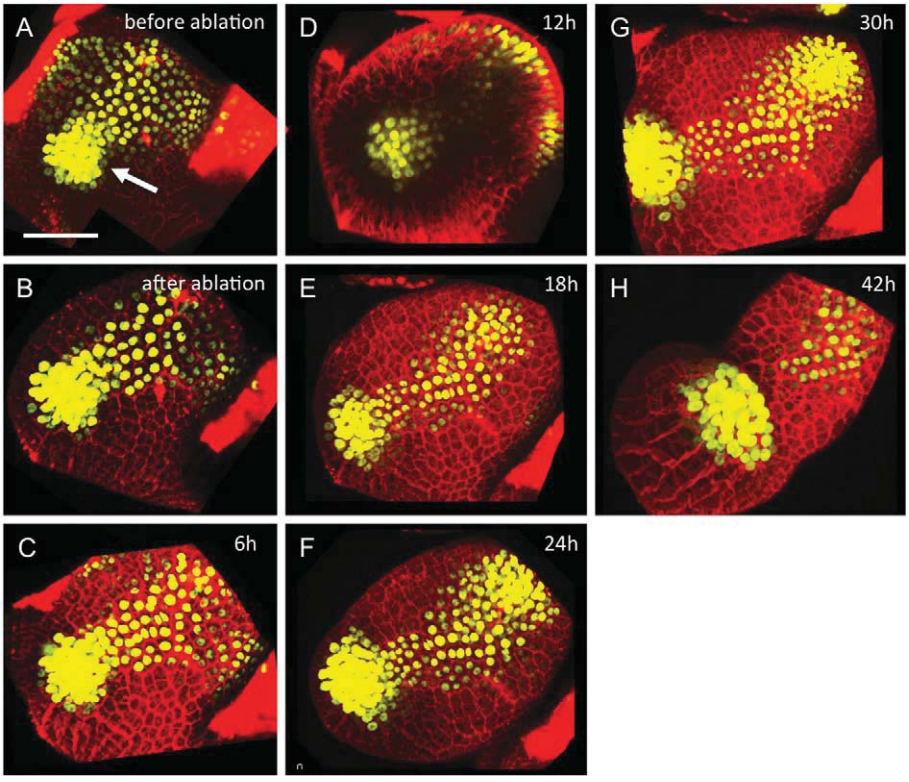

Fig. 6. Expression of DR5:YFP in a control apex without ablation. An apex of the DR5:YFP tomato line before (A) and just after (B) mock ablation, and 6 (C), 12 (D), 18 (E), 24 (F), 30 (G) and 42 (H) h after mock ablation of the midvein at P_1 (arrow). All parameters are as in Fig. 5, except that the ablation was omitted. To ensure comparable treatments, the apex was imaged before and after the mock ablation. Images represent maximum intensity projections. Scale bar: 50 µm.

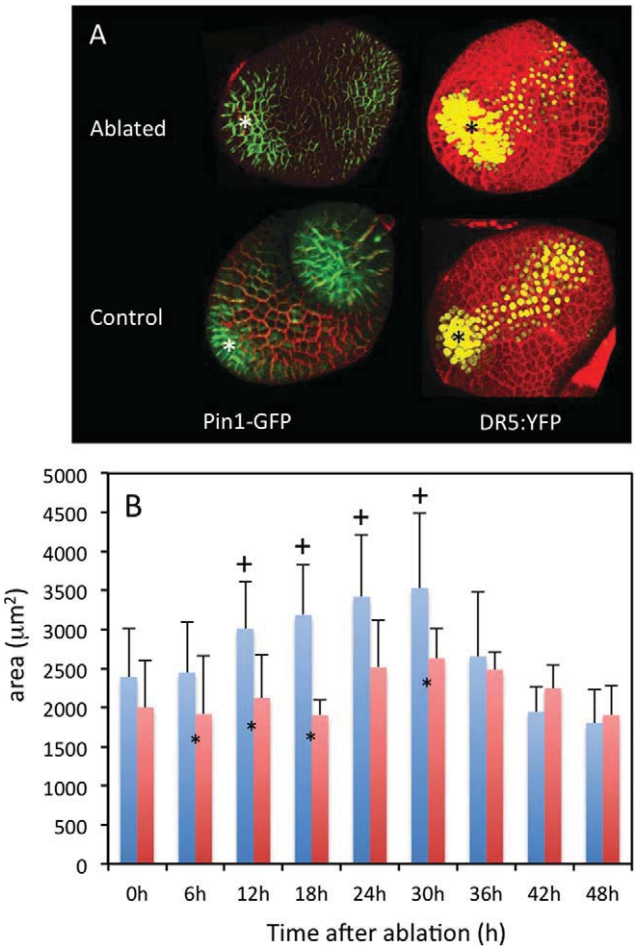

Fig. 7. Quantitative analysis of the size of the domain expressing DR5:YFP after ablation of the incipient midvein of P_1. (A) Representative images of apices 18 h after ablation (ablated) and before ablation (control) of the marker lines PIN1-GFP and DR5:YFP. Note the wider PIN1 and DR5 domain (asterisk) after ablation. Images represent maximum intensity projections. (B) Measurement of DR5:YFP apices as in A. The area of the DR5 domain was measured with ImageJ (see Materials and Methods). Error bars represent s.d. and asterisks denote significant differences (P<0.05, *t*-test) between the ablated apices (blue bars) and control apices (red bars) at the respective time points (n=7). Crosses denote significant differences (P<0.05, *t*-test) between the DR5 area of ablated apices before and after the treatment (n=7).

regulation of phyllotaxis (Kierzkowski et al., 2013). However, the substantial expression of PIN1 in the developing midvein of primordia is thought to influence phyllotactic patterning, presumably by reinforcing the gradients of auxin in L_1 (Bayer et al., 2009). Our ablation study addresses for the first time the specific role of the midvein in primordium development and patterning of the shoot apex, and thereby provides experimental evidence for models of phyllotaxis that invoke auxin drainage by the youngest primordia.

Auxin and leaf polarity

Leaves have a distinct upper and lower side, which is determined early in development by a genetic network of patterning factors (Kidner and Timmermans, 2010; Byrne, 2012). Most of these factors are transcriptional regulators that show distinct expression patterns in the upper (adaxial) or lower (abaxial) side of the leaf (Kidner and Timmermans, 2010). Besides these intrinsic determinants of leaf polarity, exogenous signals from the meristem and the subtending stem tissues influence adaxial/abaxial leaf patterning (Kidner and Timmermans, 2010). Auxin has been implicated in adaxial/abaxial organ patterning owing to the involvement of the auxin-response factors ARF3 (also known as ETTIN) and ARF4, which act in concert with the KANADI genes in the abaxial domain (Kidner and Timmermans, 2010; Byrne, 2012). In addition, low auxin levels in the adaxial domain of young primordia have recently been shown to be required for the establishment of adaxial identity (Qi et al., 2014). Interference with polar auxin transport or with auxin signaling led to polarity defects that suggest an instructive role of auxin in the establishment of dorsoventral leaf polarity (Qi et al., 2014). By contrast, midvein ablations did not affect adaxial/abaxial patterning of the primordia (Fig. 4), although they increased overall auxin levels and caused an increase in primordium width (Fig. 8). These results show that the superficial cell layers of the primordia, through which auxin is redistributed between primordia and the surrounding meristem cells (Reinhardt et al., 2003b; Qi et al., 2014), remained intact after midvein ablations.

Conclusions

Phyllotaxis is established *de novo* in the radially symmetric embryo and is maintained throughout the life cycle of the plant, although the specific phyllotactic patterns can change during vegetative development and at the onset of flowering. Phyllotaxis involves a basic auxin-related patterning mechanism and additional stabilizing factors (Prasad et al., 2011; Mirabet et al., 2012; Besnard et al., 2014), which reinforce phyllotactic patterns and allow them to be restored after perturbation of the meristem (Kuhlemeier, 2007). However, leaf initiation is also responsive to signals from the environment (Yoshida et al., 2011). The plasticity and complexity of phyllotaxis stimulated further research into its mechanistic basis, with a focus on interactions of auxin-mediated processes with biophysical patterning mechanisms (Hamant et al., 2008; Heisler et al., 2010; Kierzkowski et al., 2012; Nakayama et al., 2012). Early computational models captured the essence of phyllotactic patterning by modeling auxin transport in the L_1 surface layer of the meristem. Here, we present evidence for the involvement of internal tissues in phyllotaxis. We used a novel laser tool that allows for specific ablations of cell populations in deep tissue layers, without damage of the overlaying tissue. Our results are in agreement with a role for developing midveins as auxin drainage canals, thereby confirming their role in auxin redistribution in the apex and phyllotaxis. Thus, phyllotaxis is established through patterning mechanisms that operate simultaneously in three dimensions.

MATERIALS AND METHODS

Plant growth and *in vitro* culture

Tomato plants (*Solanum lycopersicum* cv. Moneymaker) transgenic for PIN1-GFP (Bayer et al., 2009) and *S. lycopersicum* cv. M82 transgenic for DR5:YFP were grown as described (Reinhardt et al., 1998). Shoot apices were dissected and cultured according to Fleming et al. (1997) on Murashige and Skoog (MS) medium containing 0.01 µM gibberellic acid A3 (Fluka) and 0.01 µM kinetin (Sigma). After laser ablation, apices were further cultured on synthetic medium.

In general, leaf primordia are numbered from the youngest (P_1) to older primordia (P_n). The sites of future (incipient) primordia are indicated from the first onwards with I_1-I_n. This nomenclature is defined at t_0 and maintained throughout the experiments. The cell layers of the meristem are defined from the surface towards the internal tissues with L_1 (corresponding to the epidermis), L_2 (subepidermal layer) and L_3 (the remaining internal tissues).

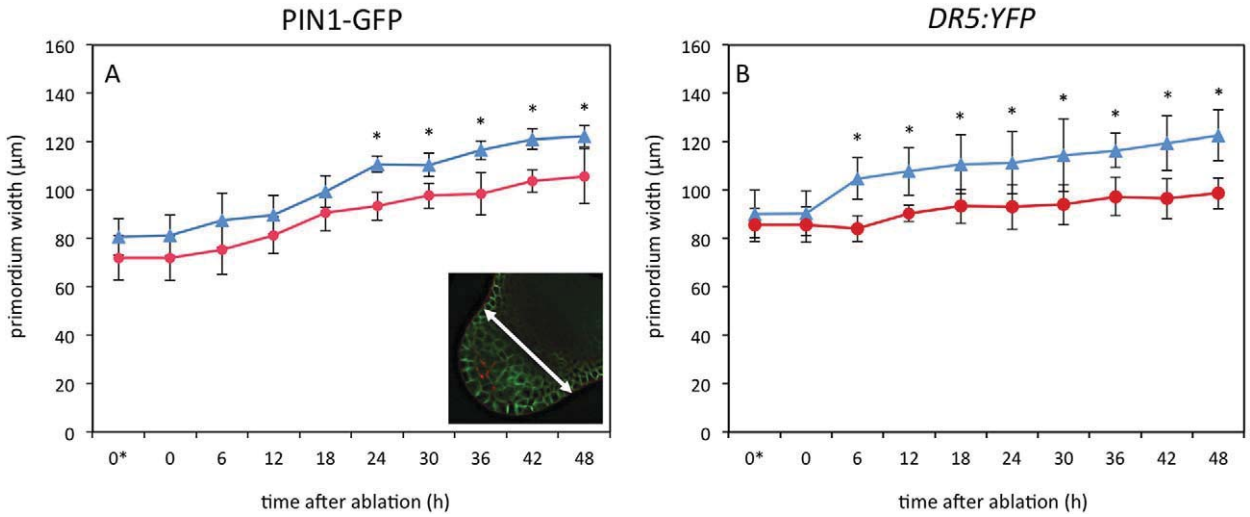

Fig. 8. Effect of ablation of the incipient midvein on the width of P_1. Apices of the marker lines PIN1-GFP (A) and DR5:YFP (B) were cultured after midvein ablation (blue) or untreated (red). Primordium width was determined as depicted in A (inset). Error bars represent s.d. and asterisks denote significant differences (P<0.05, t-test) between the primordium width of control apices and ablated apices at the respective time points (n=7).

An integrated system for microscopy and cell ablation

Laser ablation and microscopy analysis were performed with the same integrated custom-modified system. An amplified femtosecond pulse laser beam (Coherent RegA 9050, pumped by a Coherent Verdi V12 and seeded by a Coherent Mantis, wavelength 800 nm) was coupled into an inverse Nikon Ti-E A1-R MP confocal fluorescence laser-scanning microscope, using the port in which the short-pulse infrared laser beam for multiphoton scanning is usually coupled. Precise co-alignment of the confocal and the ablation modalities resulted in a tight focus with high intensity in the internal cell layers, which allowed us to ablate defined individual cells.

Laser ablation and confocal microscopy

Tomato shoot apices were maintained in their culture dishes for imaging and scanned upside down in a drop of immersion water. In order to highlight the cell walls and ablated cells the apices were submerged in 0.1% propidium iodide for 5 min before each imaging session. Confocal scanning was performed with a 1.27 NA, 60× Plan Apochromat water-immersion objective (Nikon). PIN1-GFP expression was used as a marker to identify the cells of the developing midvein in the youngest leaf primordium (P_1) for ablation (Bayer et al., 2009). Because of the integrated system, apices could be imaged immediately before and after ablation without moving. Two single shots from the amplified laser were delivered to each cell that was to be ablated. This protocol allowed for the ablation of all cells of the incipient midvein within ~2 min. The intensity of a single shot was ~0.35 GW/cm^2. After ablations, confocal imaging was performed in the plane of the ablation to determine the extent of the lesion. If necessary, ablations were repeated up to five times to achieve complete ablation of the incipient midvein. Owing to the integrated custom-built system, the entire manipulation, including two complete 3D scans and the ablation, took less than 20 min. Subsequently, the apices were cultured in their closed Petri dishes with artificial light as described. For timecourse experiments, 3D stacks were acquired every 6 h until 48 h after ablation.

Live imaging and scanning electron microscopy

For live imaging and determination of divergence angles, developing tomato apices were cultured on plates and repeatedly photographed with a Sony DKC35000 digital camera mounted on a Nikon SMZ3U stereoscope. The output was 16-bit HDR images. At the end of the treatment, apices were

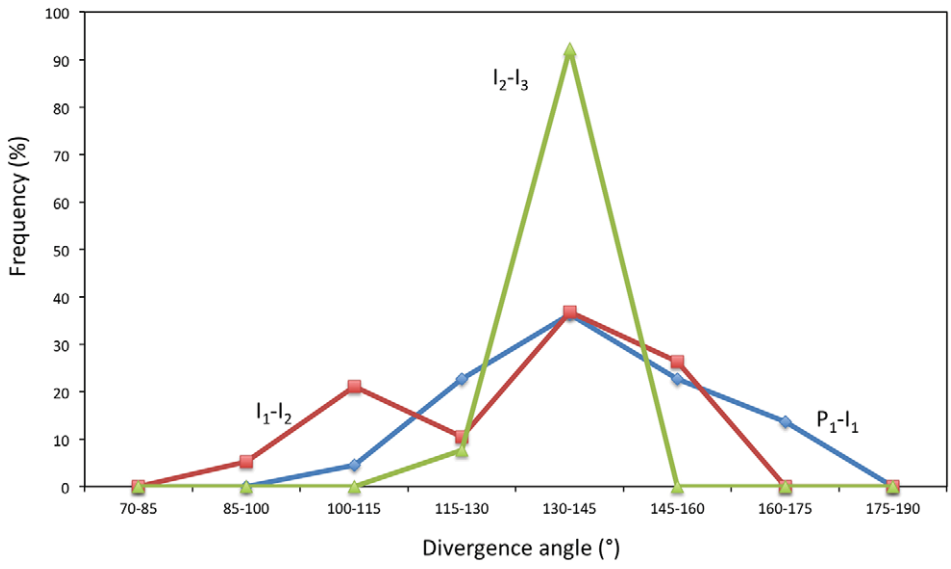

Fig. 9. Effect of ablation of the incipient midvein on leaf positioning. After ablation of the midvein of P_1, apices were further cultured and the divergence angles were determined between successive primordia and grouped into the indicated classes (n=19). Control apices were always in the class 137-145° (not shown). The first angle (P_1-I_1, blue) and the second angle (I_1-I_2, red) varied widely, whereas the third angle (I_2-I_3, green) was normal.

viewed with an S33500N variable pressure scanning electron microscope (Hitachi) equipped with a cool stage.

Quantification of DR5 expression area

Using ImageJ (NIH), the area of DR5 expression of all time points was measured in a maximum intensity projection image of the *z*-stacks by visually defining an ellipse encompassing all expressing cells.

Measurement of divergence angles

Serial live video images as well as electron micrographs of shoot apices in top view were used for the determination of consecutive divergence angles over the entire period of the experiments, as previously described (Reinhardt et al., 2005). The method first involves the precise localization of the trough between the meristem and the primordia. This is always a nearly straight tangential line that separates the two structures. From the middle of this line, we drew a perpendicular line towards the meristem center. The perpendicular lines of successive primordia cross in the central zone of the meristem, thereby defining the meristem center and the divergence angle.

Acknowledgements

We thank Naomi Ori for generously providing the tomato DR5:YFP line.

Competing interests

The authors declare no competing or financial interests.

Author contributions

D.M. and M.F. have expertise in laser technology, Y.D., D.R. and C.K. in developmental biology. Y.D. and D.M. performed the experiments; D.R., M.F. and C.K. conceived and supervised the project. All authors contributed to the interpretation of the results and the writing of the paper.

Funding

This work was supported by SystemsX.ch project 'Plant Growth in a Changing Environment' [SXRTX0-123956 and 51RT0-145716 to C.K., M.F. and D.R.] and by a grant [31003A-144136] from the Swiss National Science Foundation to C.K.

References

Bainbridge, K., Guyomarc'h, S., Bayer, E., Swarup, R., Bennett, M., Mandel, T. and Kuhlemeier, C. (2008). Auxin influx carriers stabilize phyllotactic patterning. *Genes Dev.* **22**, 810-823.

Bayer, E. M., Smith, R. S., Mandel, T., Nakayama, N., Sauer, M., Prusinkiewicz, P. and Kuhlemeier, C. (2009). Integration of transport-based models for phyllotaxis and midvein formation. *Genes Dev.* **23**, 373-384.

Benková, E., Michniewicz, M., Sauer, M., Teichmann, T., Seifertová, D., Jürgens, G. and Friml, J. (2003). Local, efflux-dependent auxin gradients as a common module for plant organ formation. *Cell* **115**, 591-602.

Berleth, T. and Sachs, T. (2001). Plant morphogenesis: long-distance coordination and local patterning. *Curr. Opin. Plant Biol.* **4**, 57-62.

Besnard, F., Refahi, Y., Morin, V., Marteaux, B., Brunoud, G., Chambrier, P., Rozier, F., Mirabet, V., Legrand, J., Laine, S. et al. (2014). Cytokinin signalling inhibitory fields provide robustness to phyllotaxis. *Nature* **505**, 417-421.

Brunoud, G., Wells, D. M., Oliva, M., Larrieu, A., Mirabet, V., Burrow, A. H., Beeckman, T., Kepinski, S., Traas, J., Bennett, M. J. et al. (2012). A novel sensor to map auxin response and distribution at high spatio-temporal resolution. *Nature* **482**, 103-106.

Byrne, M. E. (2012). Making leaves. *Curr. Opin. Plant Biol.* **15**, 24-30.

de Reuille, P. B., Bohn-Courseau, I., Ljung, K., Morin, H., Carraro, N., Godin, C. and Traas, J. (2006). Computer simulations reveal properties of the cell-cell signaling network at the shoot apex in *Arabidopsis*. *Proc. Natl. Acad. Sci. USA* **103**, 1627-1632.

Depuydt, S., Rodriguez-Villalon, A., Santuari, L., Wyser-Rmili, C., Ragni, L. and Hardtke, C. S. (2013). Suppression of *Arabidopsis* protophloem differentiation and root meristem growth by CLE45 requires the receptor-like kinase BAM3. *Proc. Natl. Acad. Sci. USA* **110**, 7074-7079.

Fleming, A. J., McQueen-Mason, S., Mandel, T. and Kuhlemeier, C. (1997). Induction of leaf primordia by the cell wall protein expansin. *Science* **276**, 1415-1418.

Furutani, M., Nakano, Y. and Tasaka, M. (2014). MAB4-induced auxin sink generates local auxin gradients in Arabidopsis organ formation. *Proc. Natl. Acad. Sci. USA* **111**, 1198-1203.

Hamant, O., Heisler, M. G., Jonsson, H., Krupinski, P., Uyttewaal, M., Bokov, P., Corson, F., Sahlin, P., Boudaoud, A., Meyerowitz, E. M. et al. (2008). Developmental patterning by mechanical signals in *Arabidopsis*. *Science* **322**, 1650-1655.

Heisler, M. G., Ohno, C., Das, P., Sieber, P., Reddy, G. V., Long, J. A. and Meyerowitz, E. M. (2005). Patterns of auxin transport and gene expression during primordium development revealed by live imaging of the Arabidopsis inflorescence meristem. *Curr. Biol.* **15**, 1899-1911.

Heisler, M. G., Hamant, O., Krupinski, P., Uyttewaal, M., Ohno, C., Jönsson, H., Traas, J. and Meyerowitz, E. M. (2010). Alignment between PIN1 polarity and microtubule orientation in the shoot apical meristem reveals a tight coupling between morphogenesis and auxin transport. *PLoS Biol.* **8**, e1000516.

Jönsson, H., Heisler, M. G., Shapiro, B. E., Meyerowitz, E. M. and Mjolsness, E. (2006). An auxin-driven polarized transport model for phyllotaxis. *Proc. Natl. Acad. Sci. USA* **103**, 1633-1638.

Kang, J. and Dengler, N. (2004). Vein pattern development in adult leaves of Arabidopsis thaliana. *Int. J. Plant Sci.* **165**, 231-242.

Kang, J., Tang, J., Donnelly, P. and Dengler, N. (2003). Primary vascular pattern and expression of ATHB-8 in shoots of Arabidopsis. *New Phytol.* **158**, 443-454.

Kang, J., Park, J., Choi, H., Burla, B., Kretzschmar, T., Lee, Y. and Martinoia, E. (2011). Plant ABC transporters. *Arabidopsis Book* 9, e0153.

Kidner, C. A. and Timmermans, M. C. P. (2010). Signaling sides: adaxial-abaxial patterning in leaves. In *Plant Development* (ed. M. C. P. Timmermans), pp. 141-168. San Diego: Academic Press.

Kierzkowski, D., Nakayama, N., Routier-Kierzkowska, A.-L., Weber, A., Bayer, E., Schorderet, M., Reinhardt, D., Kuhlemeier, C. and Smith, R. S. (2012). Elastic domains regulate growth and organogenesis in the plant shoot apical meristem. *Science* **335**, 1096-1099.

Kierzkowski, D., Lenhard, M., Smith, R. and Kuhlemeier, C. (2013). Interaction between meristem tissue layers controls phyllotaxis. *Dev. Cell* **26**, 616-628.

Kirchoff, B. K. (1984). On the relationship between phyllotaxy and vasculature: a synthesis. *Bot. J. Linn. Soc.* **89**, 37-51.

Krecek, P., Skupa, P., Libus, J., Naramoto, S., Tejos, R., Friml, J. and Zazimalova, E. (2009). The PIN-FORMED (PIN) protein family of auxin transporters. *Genome Biol.* **10**, 249.

Kuhlemeier, C. (2007). Phyllotaxis. *Trends Plant Sci.* **12**, 143-150.

Larson, P. R. (1975). Development and organization of the primary vascular system in *Populus deltoides* according to phyllotaxy. *Am. J. Bot.* **62**, 1084-1099.

Mirabet, V., Besnard, F., Vernoux, T. and Boudaoud, A. (2012). Noise and robustness in phyllotaxis. *PLoS Comput. Biol.* **8**, e1002389.

Nakayama, N., Smith, R. S., Mandel, T., Robinson, S., Kimura, S., Boudaoud, A. and Kuhlemeier, C. (2012). Mechanical regulation of auxin-mediated growth. *Curr. Biol.* **22**, 1468-1476.

Pilkington, M. (1929). The regeneration of the stem apex. *New Phytol.* **28**, 37-53.

Prasad, K., Grigg, S. P., Barkoulas, M., Yadav, R. K., Sanchez-Perez, G. F., Pinon, V., Blilou, I., Hofhuis, H., Dhonukshe, P., Galinha, C. et al. (2011). Arabidopsis PLETHORA transcription factors control phyllotaxis. *Curr. Biol.* **21**, 1123-1128.

Qi, J., Wang, Y., Yu, T., Cunha, A., Wu, B., Vernoux, T., Meyerowitz, E. and Jiao, Y. (2014). Auxin depletion from leaf primordia contributes to organ patterning. *Proc. Natl. Acad. Sci. USA* **111**, 18769-18774.

Reinhardt, D. (2005). Phyllotaxis - a new chapter in an old tale about beauty and magic numbers. *Curr. Opin. Plant Biol.* **8**, 487-493.

Reinhardt, D., Wittwer, F., Mandel, T. and Kuhlemeier, C. (1998). Localized upregulation of a new expansin gene predicts the site of leaf formation in the tomato meristem. *Plant Cell* **10**, 1427-1437.

Reinhardt, D., Mandel, T. and Kuhlemeier, C. (2000). Auxin regulates the initiation and radial position of plant lateral organs. *Plant Cell* **12**, 507-518.

Reinhardt, D., Frenz, M., Mandel, T. and Kuhlemeier, C. (2003a). Microsurgical and laser ablation analysis of interactions between the zones and layers of the tomato shoot apical meristem. *Development* **130**, 4073-4083.

Reinhardt, D., Pesce, E.-R., Stieger, P., Mandel, T., Baltensperger, K., Bennett, M., Traas, J., Friml, J. and Kuhlemeier, C. (2003b). Regulation of phyllotaxis by polar auxin transport. *Nature* **426**, 255-260.

Reinhardt, D., Frenz, M., Mandel, T. and Kuhlemeier, C. (2005). Microsurgical and laser ablation analysis of leaf positioning and dorsoventral patterning in tomato. *Development* **132**, 15-26.

Robert, H. S. and Offringa, R. (2008). Regulation of auxin transport polarity by AGC kinases. *Curr. Opin. Plant Biol.* **11**, 495-502.

Sachs, T. (1981). The control of the patterned differentiation of vascular tissues. *Adv. Bot. Res. Inc. Adv. Plant Pathol.* **9**, 151-262.

Sauer, M., Balla, J., Luschnig, C., Wisniewska, J., Reinöhl, V., Friml, J. and Benkova, E. (2006). Canalization of auxin flow by Aux/IAA-ARF-dependent feedback regulation of PIN polarity. *Genes Dev.* **20**, 2902-2911.

Sawchuk, M. G., Edgar, A. and Scarpella, E. (2013). Patterning of leaf vein networks by convergent auxin transport pathways. *PLoS Genet.* **9**, e1003294.

Scarpella, E., Francis, P. and Berleth, T. (2004). Stage-specific markers define early steps of procambium development in *Arabidopsis* leaves and correlate termination of vein formation with mesophyll differentiation. *Development* **131**, 3445-3455.

Scarpella, E., Barkoulas, M. and Tsiantis, M. (2010). Control of leaf and vein development by auxin. *Cold Spring Harb. Perspect. Biol.* **2**, a001511.

Schoute, J. C. (1913). Beiträge zur Blattstellungslehre. *Extr. Rec. Trav. Bot. Néerl.* **10**, 153-235.

Shani, E., Ben-Gera, H., Shleizer-Burko, S., Burko, Y., Weiss, D. and Ori, N. (2010). Cytokinin regulates compound leaf development in tomato. *Plant Cell* **22**, 3206-3217.

Smith, R. S., Kuhlemeier, C. and Prusinkiewicz, P. (2006a). Inhibition fields for phyllotactic pattern formation: a simulation study. *Can. J. Bot. Rev. Can. Bot.* **84**, 1635-1649.

Smith, R. S., Guyomarc'h, S., Mandel, T., Reinhardt, D., Kuhlemeier, C. and Prusinkiewicz, P. (2006b). A plausible model of phyllotaxis. *Proc. Natl. Acad. Sci. USA* **103**, 1301-1306.

Snow, M. and Snow, R. (1931). Experiments on phyllotaxis. I. The effect of isolating a primordium. *Philos. Trans. R. Soc. Lond. B Biol. Sci.* **221**, 1-43.

Snow, M. and Snow, R. (1933). Experiments on phyllotaxis. II. The effect of displacing a primordium. *Philos. Trans. R. Soc. Lond. B Biol. Sci.* **222**, 353-400.

Sussex, I. M. (1951). Experiments on the cause of dorsiventrality in leaves. *Nature* **167**, 651-652.

Swarup, R. and Peret, B. (2012). AUX/LAX family of auxin influx carriers—an overview. *Front. Plant Sci.* **3**, 225.

van den Berg, C., Willemsen, V., Hage, W., Weisbeek, P. and Scheres, B. (1995). Cell fate in the *Arabidopsis* root meristem determined by directional signalling. *Nature* **378**, 62-65.

van den Berg, C., Willemsen, V., Hendriks, G., Weisbeek, P. and Scheres, B. (1997). Short-range control of cell differentiation in the *Arabidopsis* root meristem. *Nature* **390**, 287-289.

Xu, J., Hofhuis, H., Heidstra, R., Sauer, M., Friml, J. and Scheres, B. (2006). A molecular framework for plant regeneration. *Science* **311**, 385-388.

Yoshida, S., Mandel, T. and Kuhlemeier, C. (2011). Stem cell activation by light guides plant organogenesis. *Genes Dev.* **25**, 1439-1450.

Zazimalova, E., Murphy, A. S., Yang, H., Hoyerova, K. and Hosek, P. (2010). Auxin transporters—why so many? *Cold Spring Harb. Perspect. Biol.* **2**, a001552.